

# Seismic Performance Evaluation of Apartment Buildings with Central Core

Joonho Lee, Seungho Han, and Jinkoo Kim<sup>†</sup>

*Dept. of Civil and Architectural Engineering, Sungkyunkwan University, Suwon, Korea*

---

## Abstract

In this study the seismic performances of reinforced concrete apartment buildings with Y- and box-shaped plans having central core are investigated. Three types of model structures are designed for each shape depending on the amount of shear partition walls: structures with all shear walls, structures with all columns except the core walls, and structures with shear walls and columns combined. The required amount of concrete to satisfy the specified design loads is the largest in the all shear wall structures, and decreases as more and more shear walls are replaced with columns. The amount of re-bars increased significantly in the flat plate structures. According to nonlinear static and dynamic analysis results, the structures with all shear walls and all columns turn out to have the largest and the smallest strengths, respectively. However it is observed that even the all-column structures with shear core have proper load resisting capacity for design level seismic load.

**Keywords:** Seismic performance evaluation, Fragility analysis, Incremental dynamic analysis

---

## 1. Introduction

Shear wall systems have been a popular choice in seismic design of building structures due mainly to the facts that they are both efficient in terms of construction cost and effective in minimizing earthquake damage. Properly designed shear walls have shown good seismic performance in many experiments (Gupta and Rangan 1998; Thomsen and Wallace, 2004; Yun et al., 2004; Dazio et al., 2009). Analytical studies of shear wall structures also have been performed by many researchers (Kim et al., 2005; Mo et al., 2008; Kara and Dundar, 2009; Wdowicki and Wdowicka, 2012; Lee and Kim, 2013).

One of the new paradigms of the twenty first century construction industry is to design structures more sustainable and resource efficient. In Korea many apartment buildings composed mainly of vertical shear walls have been demolished not because the structures were old and weakened beyond repair but because the plan layouts divided into many small spaces by shear walls did not fit the changed life style of residences who prefer large open spaces. To enhance the ease of remodeling of residential buildings, Korean government provides various incentives for apartment buildings designed with spatial flexibility. This can be achieved by replacing the interior shear walls of apartment buildings with columns and removable partitions so that new residence can reshape the interior spaces as they like. However the removal of shear walls

may result in insufficient lateral load-resisting system against seismic load.

This study investigates the seismic performance of apartment buildings with central RC core and transverse shear partition walls. Both Y- and Box-shaped structures in plan, which are common shapes of high-rise residential buildings currently built in Korea, were designed using the same design loads for comparison. At each shape three different variations were made depending on the amount of shear partition walls. The first type of model structure was designed only with shear partition walls in addition to the central core. The second type was designed with a part of transverse shear walls replaced by columns. The third analysis model structure was designed with all transverse shear walls replaced by columns. Lateral loads are resisted by the central core and the column-slab system surrounding the core. Nonlinear static and dynamic analyses were carried out to obtain ultimate strength and collapse mechanism of the model structures. The probability of failure of the structure with smallest strength and stiffness was obtained by fragility analysis using 22 pairs of far field earthquake records. The amount of concrete and reinforcing steel required to design the model structures per the current design code were also compared.

## 2. Design and Analysis Modeling of Example Structures

The analysis model structures are the twenty-story Y-shaped and box-shaped reinforced concrete (RC) buildings composed of four apartment units per floor. To study the seismic performance of the structures with different

---

<sup>†</sup>Corresponding author: Jinkoo Kim  
Tel: +82-31-290-7563; Fax: +82-31-290-7570  
E-mail: jkim12@skku.edu

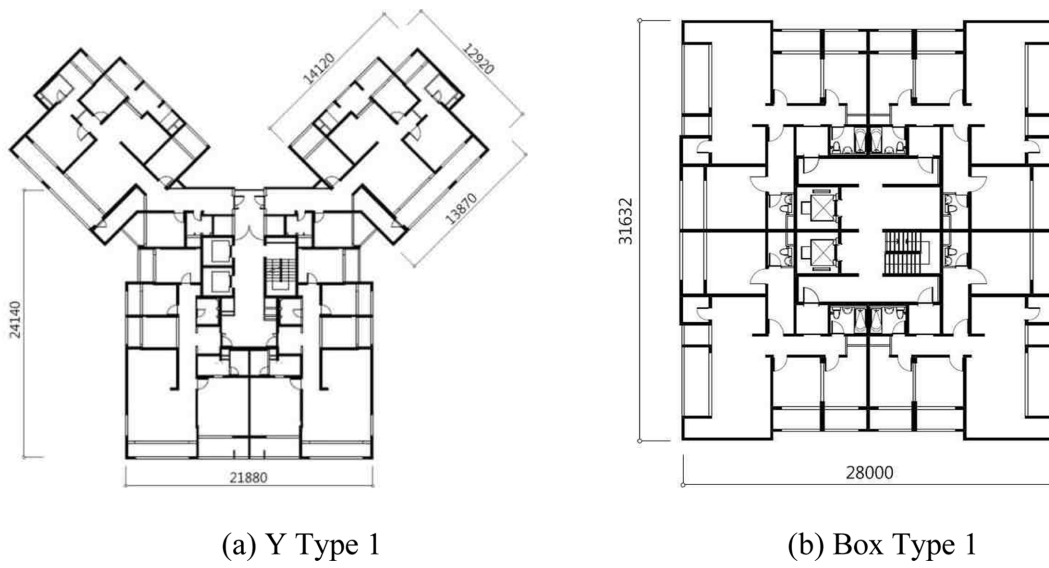


**Figure 1.** Structural plans of analysis model structures (type 1).

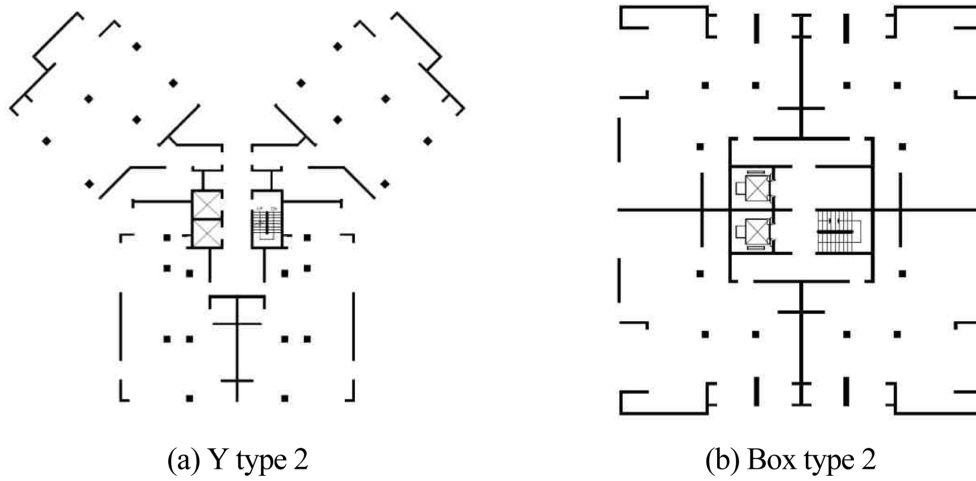


**Figure 2.** Structural plans of flat plate wall system (type 2).

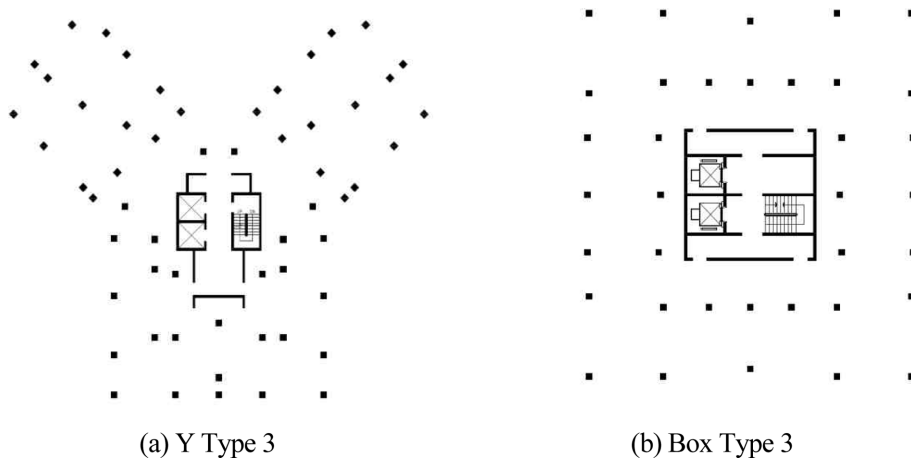


**Figure 3.** Structural plans of flat plate system (type 3).

spatial variability, the following three types of analysis model structures were prepared: the structures with transverse shear walls (Type-1); the structures with part of the shear walls replaced by columns; and the structures with all transverse shear walls replaced by columns (Type-3). Fig. 1 shows the structural plans of the Type-1 analysis model structures composed of transverse shear walls, which are typical structural forms of high-rise apartment buildings currently built in Korea. Fig. 2 shows the plan shape of Type-2 structures in which short transverse shear walls inside of each unit were replaced by columns. In Type-3 structures depicted in Fig. 3 all shear walls except the core walls were replaced by columns, in which two apartment units can be combined into one large unit. All model structures have the same story height of 3 m. The Box-shaped structures have overall plan dimensions of  $28 \text{ m} \times 32.6 \text{ m}$ , and the Y-shaped structures were designed to have similar plan area.

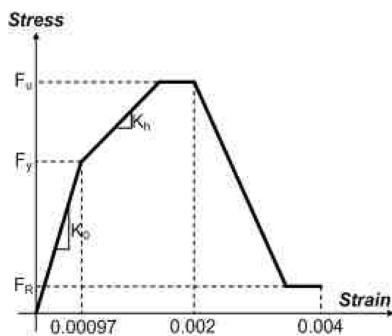
The analysis model structures were designed with both gravity and lateral loads such as wind and seismic loads. The dead load used for design is  $7 \text{ kN/m}^2$  which includes the weight of 210 mm-thick slab and the panel heating system, and the live load is  $2 \text{ kN/m}^2$ . The design wind load was computed based on the basic wind speed of 30 m/sec as specified in the Korean Building Code (KBC 2009). The seismic loads were evaluated using the seismic coefficients  $S_{DS}$  and  $S_{D1}$  equal to 0.37 and 0.15, respectively, in the IBC (International Building Code) format (IBC 2007). The response modification coefficient (R-factor) for Type-1 structures is 4.0 which corresponds to the R-factor for ordinary RC shear wall structures in the category of Bearing Wall Systems in KBC 2009. The R-factor of 5.0 was used for Type-2 and Type-3 structures, which were considered as ordinary RC shear wall structures in the Building Frame Systems. The structures were assumed to be built on a site with Class B soil defined in KBC 2009. The design base shears for seismic load turned out to be larger than those for wind load in all model structures. In the Y-shaped structures the thickness of the core wall is 200 mm, 250 mm, and 300 mm in the

**Table 1.** Design base shears and modal characteristics of the model structures

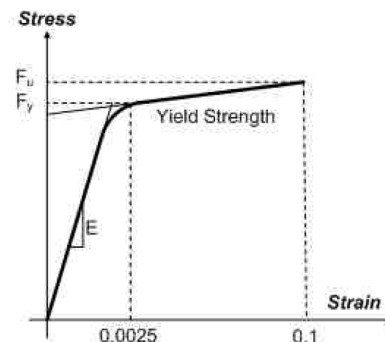
Model structures	$V_d(\text{kN})$	Mode 1		
		Period (sec.)	Modal mass (%)	
Y - Type1	X-dir	7357.7	1.78	51.78
	Y-dir	7380.5	1.32	63.83
Y - Type 2	X-dir	5219.1	2.30	56.10
	Y-dir	5218.2	1.32	65.18
Y - Type 3	X-dir	4493.2	3.18	46.43
	Y-dir	4479.6	1.59	65.53
Box - Type 1	X-dir	7138.5	1.18	64.51
	Y-dir	7388.3	1.11	65.03
Box - Type 2	X-dir	5293.3	1.34	64.38
	Y-dir	5315.4	1.32	64.72
Box - Type 3	X-dir	4736.6	1.62	66.27
	Y-dir	4747.3	1.38	65.70

Type-1, Type-2, and Type-3 structures, respectively. In the box-shaped structures the thickness of the Type-3 structure was increased to 350 mm while those of Type-1 and Type-2 structures are the same with the thicknesses of the Y-shaped structures. The transverse shear walls have the uniform thickness of 200 mm. The model structures were designed in such a way that the strength ratios (the ratios of demand and capacity) of shear walls and columns were maintained between 0.7 and 0.8 in all model structures.

Table 1 shows the design base shear and the dynamic characteristics of model structures such as fundamental period and modal mass. It can be observed that the design base shear is the largest in the Type-1 structures and is the smallest in the Type-3 structures in which all transverse shear walls were replaced with columns. This is related to the fact that the fundamental period increases as the amount of transverse shear wall decreases. The fundamental modal mass, however, did not depend on the amount of transverse shear walls. The thickness of floor slabs is 210 mm which is the minimum value for shear wall apartment buildings to prevent transmission of excessive noise and



(a) Concrete



(b) Re-bar

**Figure 4.** Stress-strain relationships of structural materials.

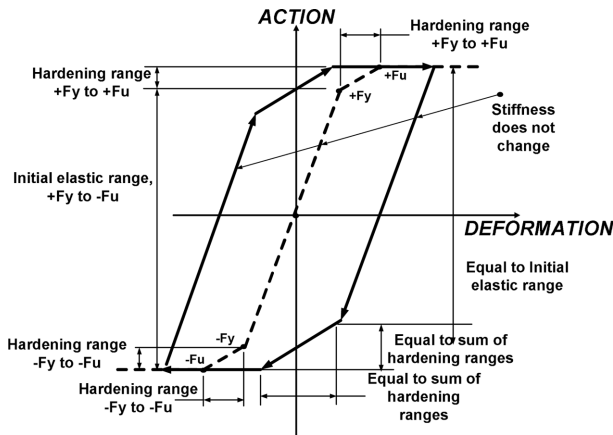


**Figure 5.** Hysteresis loop of columns provided in the Perform 3D.

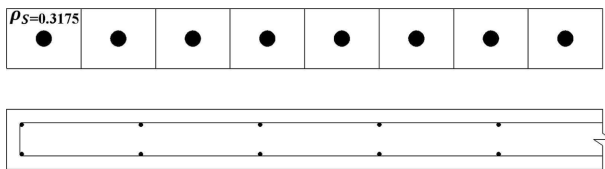


**Figure 6.** Auto-sized fiber section for shear wall elements.

vibration through the slabs.

The stress-strain relationships of concrete and reinforcing steel were defined as tri-linear and bi-linear lines, respectively, as shown in Fig. 4 based on the material model of Paulay and Priestley (1992) without confinement effect. In the model the ultimate strength and yield strength of concrete are 27 MPa and 18 MPa, respectively, and the residual strength was defined as 20% of the ultimate strength. The strain at the ultimate strength is 0.002, and the ultimate strain is defined as 0.004. For reinforcing steel,  $F_y$  and  $F_u$  are 400 MPa and 480 MPa, respectively. The shear walls were modeled by the Shear Wall fiber elements in the Perform 3D (2006) as shown in Fig. 6. The axial bending behavior was modeled by vertical fiber elements, and the transverse stiffness of the wall and the out-of-plane bending stiffness were assumed to be elastic. For reinforced concrete columns, the “FEMA Column, Concrete Type” element in Perform 3D shown in Fig. 5 was used to model inelastic bending in concrete columns, based on an interpretation of the ASCE/SEI 41-06 Table 6-8. To define a column plastic hinge, a moment-axial capacity interaction curve was calculated using the expected material properties. The back bone curve is tri-linear and

**Table 2.** Maximum roof displacement under the design wind load (H: building height)

	X-dir	Y-dir
Y - Type 1	H / 2431	H / 4337
Y - Type 2	H / 1276	H / 3897
Y - Type 3	H / 533	H / 2248
Box - Type 1	H / 4434	H / 5845
Box - Type 2	H / 3102	H / 3646
Box - Type 3	H / 1963	H / 2982

**Table 3.** Maximum inter-story drift under design seismic load

	X-dir	Y-dir
Y - Type 1	0.0022	0.0016
Y - Type 2	0.0022	0.0013
Y - Type 3	0.0028	0.0016
Box - Type 1	0.0015	0.0013
Box - Type 2	0.0013	0.0013
Box - Type 3	0.0015	0.0013

$M_y$  was assumed to be 80% of  $M_u$ . The unloading stiffness was modeled to be equal to the initial elastic stiffness. The energy degradation factor was set to be zero, which resulted in the same unloading and reloading lines.

Table 2 shows the maximum roof displacements of model structures subjected to the design wind load. As expected the maximum displacement increased as the amount of shear wall decreased. However even the largest displacement occurred in the Y-Type 3 structure was less than 1/500 of the total height and was considered to be adequate. The maximum inter-story drifts of the model structures subjected to design seismic loads were presented in Table 3, where it can be observed that the maximum story drifts are well within the limit state of 1.5% of the story height required by the KBC 2009 design code. Table 4 compares the quantities of the concrete and re-bars used in the design of shear walls and columns in the analysis model structures. It can be observed that the required amount of concrete is largest in the Type-1 structures with largest amount of shear walls and is smallest in the Type 3 structures with no transverse shear walls in both Y- and Box-shaped structures. The steel tonnage is smallest in the Type-2 structures in both Y- and Box-shaped structures. In the Y-shaped structures the required weight of re-bar is largest in the Type-3 structure which is subjected to large torsional deformation. In the Box-shaped structures the amount of re-bar in the Type-1 structure is slightly larger than that in the Type-3 struc-

**Table 4.** Quantity of structural materials used in the shear walls and columns

Material	Y-shaped			Box shaped		
	Type -1	Type -2	Type -3	Type -1	Type -2	Type -3
Concrete (m <sup>3</sup> )	4,057	2,803	1,816	4,090	3,085	2,246
Re-bar (kN)	3,810	3,275	7,274	3,214	2,275	3,119

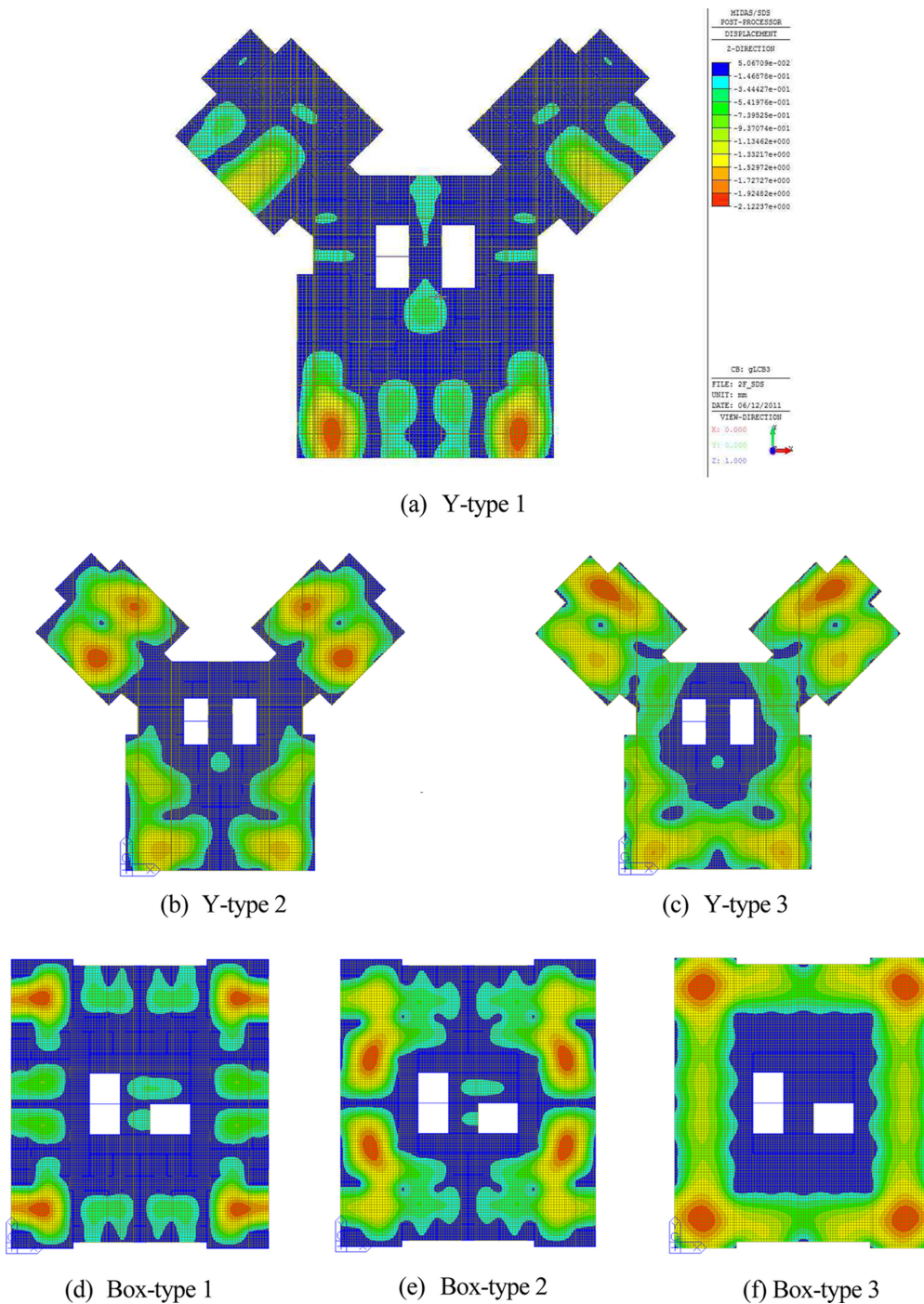


Figure 7. Vertical deflection of slabs under service loads.

ture. Based on the amount of structural materials required to resist the given design loads, the Type-2 structures with mixed use of shear walls and columns seem to be the most efficient.

Figure 7 shows the stress distribution of floor slabs of model structures under service gravity loads, and the magnitudes of maximum deflections are shown in Table 5. It can be observed that the vertical deflection is the largest in the Type 3 model structures with all transverse shear

Table 5. Maximum deflection of slab under service loads

Type	Maximum deflection
Y - Type 1	1.278mm
Y - Type 2	3.104mm
Y - Type 3	3.998mm
Box - Type 1	0.936mm
Box - Type 2	1.580mm
Box - Type 3	3.819mm

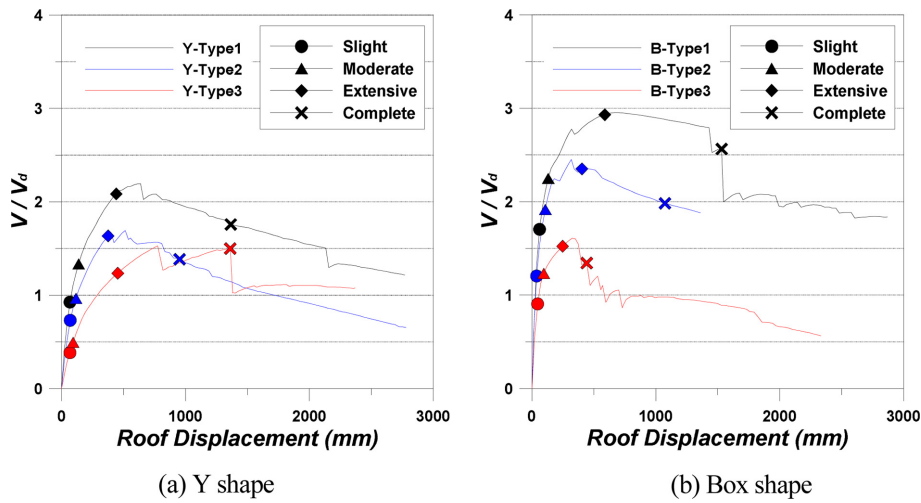


Figure 8. Pushover curves of the model structures.

Table 6. Maximum inter-story drift ratios of analysis model structures

	Slight Damage	Moderate Damage	Extensive Damage	Complete Damage
Y - Type 1	0.001468	0.002962	0.009364	0.025254
Y - Type 2	0.001523	0.002503	0.008089	0.018801
Y - Type 3	0.001391	0.001891	0.009380	0.030358
Box - Type 1	0.001306	0.002794	0.011595	0.029278
Box - Type 2	0.000823	0.002309	0.008044	0.019408
Box - Type 3	0.000930	0.001928	0.004901	0.010439

walls replaced by columns. However they turned out to satisfy the limit state for vertical deflection under service load specified in the KBC 2009.

### 3. Seismic Performance of the Model Structures

#### 3.1. Pushover analysis results

The seismic performances of the model structures were evaluated using the Perform-3D. Nonlinear static pushover analyses were carried out along the principal axis of the structures until the maximum displacements reach 5% of the total height to identify nonlinear force-displacement relationships of the model structures. The lateral story forces were determined in proportion to the fundamental mode shapes. Fig. 8 shows the pushover curves of the model structures, where the vertical axis represents the applied base shear,  $V$ , normalized by the design base shear,  $V_d$ , and the horizontal axis represents the roof displacement. The pushover analysis results of the Y-shape structure were already presented in Kim et al. (2013). The points of four damage states specified in the Korea National Emergency Management Agency are also marked on the curves. The damage states of structures were divided into four levels such as Slight, Moderate, Extensive, and Complete. The states of ‘Slight Damage’ and ‘Moderate Damage’ were defined as the spectral dis-

placements corresponding to 70% and 100% of yield point, respectively. The ‘Extensive Damage’ was defined as the quarter point from ‘Moderate’ to ‘Complete’ damage. The ‘Complete Damage’ was the spectral displacement at which the strength decreased to 80% of the maximum strength. Table 6 shows the maximum inter-story drift ratios of the model structures at each damage state. It can be observed that the maximum strength is the highest in the Type-1 structures with largest amount of shear walls, and decreases as the amount of shear wall decreases. The strength is generally higher in the Box-shaped structures than in the Y-shaped structures. In the Y-shaped models the overstrength ranges from 1.5 (Type-3) to 2.2 (Type-2), and in the Box-shaped structures the overstrength ranges from 1.6 in the Type-3 model to 3.0 in the Type-1 model. Both in the Y- and Box-shaped structures, the Type-3 structures show smallest strength. It is observed that in the Type-1 and Type-2 structures plastic hinges form first in the first story transverse shear walls and spread to shear walls in the higher stories. In the Type-3 structures plastic hinges are concentrated in the lower story core walls and the structures experience relatively less energy dissipation and fail at smaller maximum displacements.

#### 3.2. Nonlinear dynamic analysis results

The seismic performances of the model structures were

**Table 7.** List of earthquake ground motions used in the dynamic analysis

Ground motion record	Duration (sec)	PGA (g)
Northridge	29.99	0.52
Imperial Valley	99.92	0.35
Kobe, Japan	40.96	0.51
Loma Prieta	39.95	0.53
Superstition Hills	22.30	0.45
Chi-Chi, Taiwan	90.00	0.44
San Fernando	28.00	0.21

also evaluated through nonlinear dynamic analyses using the seven earthquake records shown in Table 7 selected from earthquake records provided by the Pacific Earthquake Engineering Research Center (PEER). The selected records were scaled to fit the design spectrum for earthquake load with return period of 2,400 years specified in the KBC 2009 in such a way that the pseudo accelerations of the records at the natural period of a model structure were equal to the spectral acceleration of the design spectrum at the same natural period. Fig. 9 shows the response spectra of the seven earthquake records, the design spectrum of the KBC 2009, and the median response spectrum. The scale factors used to scale the earthquake records are shown in Table 8. In all cases damping ratio was assumed to be 5% of the critical damping. Fig. 10

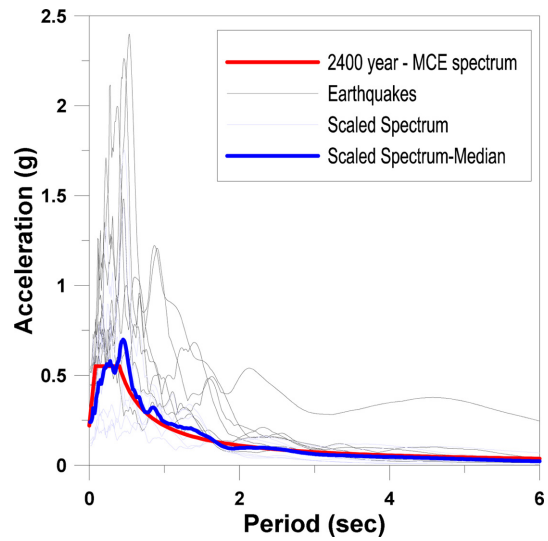


**Figure 9.** Response spectra of seven earthquake records and maximum considered earthquake spectrum.

depicts the mean inter-story drifts of the model structures. In the Y-shaped structures, the inter-story drifts of the Type-3 structure with least number of shear walls are almost twice as high as those of the Type-1 structures. In the Box shaped structures the differences in inter-story

**Table 8.** Scale factors of earthquake ground motions

Ground motion record	Y Type -1	Y Type -2	Y Type -3	Box Type -1	Box Type -2	Box Type -3
Northridge	0.2645	0.6329	0.8852	0.2176	0.2271	0.2521
Imperial Valley	0.3029	0.5061	0.6516	0.6726	0.5466	0.3826
Kobe, Japan	0.7755	0.6009	1.1277	0.6904	0.9496	0.7667
Loma Prieta	0.4063	0.7863	1.3113	0.3946	0.2739	0.2494
Superstition Hills	0.9688	0.6866	0.7194	0.5092	0.5424	0.7652
Chi-Chi, Taiwan	0.2759	0.1952	0.2447	0.3084	0.4003	0.3626
San Fernando	1.1908	1.3894	0.7744	0.8340	0.6766	0.6871

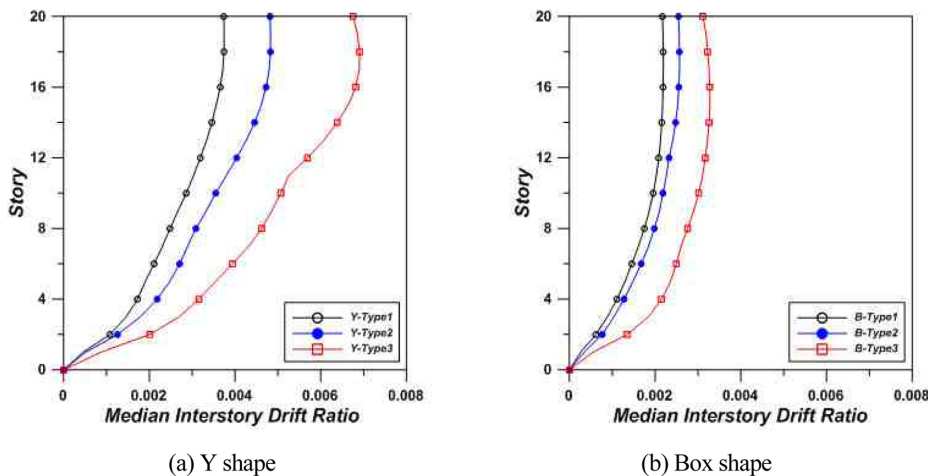


**Figure 10.** Mean inter-story drifts of analysis models obtained from non-linear dynamic analysis using seven earthquake records.

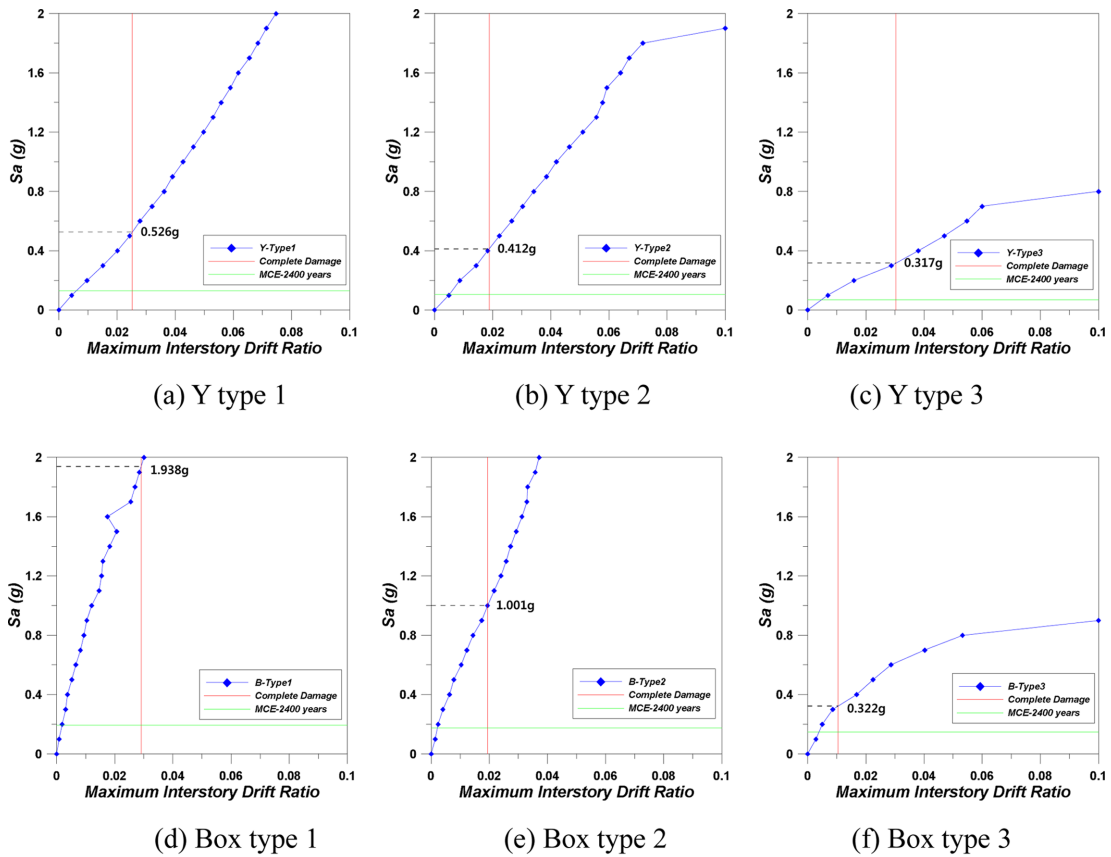


Figure 11. Maximum inter-story drifts of analysis models obtained from incremental dynamic analysis.

drifts is smaller than those in the Y-shaped structures due to higher torsional rigidity. It can be observed that the maximum inter-story drifts of the model structures subjected to design level earthquake ground excitation are significantly smaller than the limit state of 1.5% of story height specified in the design code.

3.3. Incremental dynamic analysis results

In this section the incremental dynamic analyses of the model structures are performed using the Superstition Hills earthquake record. A series of nonlinear dynamic analysis are carried out by increasing the response spectral value corresponding to the fundamental natural period of each structure by 0.1 g. The response spectra ( $S_a$ ) and the corresponding inter-story drifts obtained from the incremental dynamic analyses are shown in Fig. 11. The MCE-level seismic intensity in Seoul area with return period of 2,400 years and the inter-story drifts at the complete damage state obtained from the pushover analyses are also shown in the figures. The analysis results show that in the Y-Type 1 structure, which is the all-shear wall structure, the complete damage state was reached at  $S_a=0.526$  g. The earthquake intensity at the same damage state is reduced to 0.412 g in Type 2 structure and to 0.317 g in the Type 3 structure. Similar trend can be observed in the Box type structures, except that the strengths at the com-

plete damage state are generally higher than those of the Y-Type structures, especially in the structures with shear partition walls. As expected the strength at the damage state keeps decreasing as more and more shear walls are replaced by columns. However in all cases the strengths at the complete damage states are significantly higher than those corresponding to the MCE-level earthquake.

4. Seismic Performance Evaluation Based on the ATC-63 Procedure

In this section the seismic performance evaluation procedure proposed in the ATC-63 is applied to the Y-Type 3 model structure which turns out to have the smallest strength and stiffness. The ATC-63 recommends a methodology for quantifying building system performance and response parameters for use in seismic design. In the ATC-63 nonlinear dynamic analyses are used to assess median collapse capacities, and collapse margin ratios. Nonlinear incremental dynamic analyses were conducted using the 22 pairs of far-field earthquake records obtained from the PEER Center to establish the median collapse capacity and collapse margin ratio ( $CMR$ ) for the analysis model. The ratio between the median collapse intensity,  $\hat{S}_{CT}$ , and the MCE intensity,  $S_{MTB}$  is defined as the collapse margin ratio ( $CMR$ ), which is the primary parameter used to cha-

racterize the collapse safety of the structure.

$$CMR = \frac{\hat{S}_{CT}}{S_{MT}} = \frac{SD_{CT}}{SD_{MT}} \quad (1)$$

The median collapse capacity corresponds to a 50% probability of collapse. To account for the effect of spectral shape in determination of the collapse margin ratio, the spectral shape factors,  $SSF$ , which depend on fundamental period,  $T$ , and ductility capacity,  $\mu_C$ , are used to adjust collapse margin ratios. The adjusted collapse margin ratio (ACMR) is obtained by multiplying tabulated  $SSF$  values with the collapse margin ratio that was predicted using the Far-Field record set.

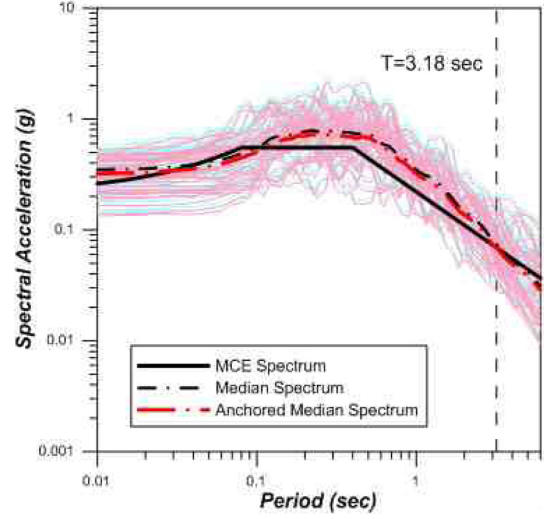
Acceptable values of adjusted collapse margin ratio are based on total system collapse uncertainty,  $\beta_{TOT}$  and established values of acceptable probabilities of collapse. They are based on the assumption that the distribution of collapse level spectral intensities is lognormal, with a median value,  $\hat{S}_{CT}$ , and a lognormal standard deviation equal to the total system collapse uncertainty,  $\beta_{TOT}$ .

$$\beta_{TOT} = \sqrt{\beta_{RTR}^2 + \beta_{DR}^2 + \beta_{TD}^2 + \beta_{MDL}^2} \quad (2)$$

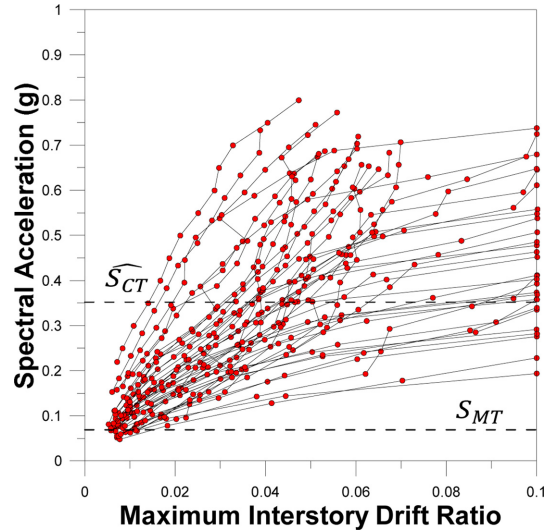
The total system collapse uncertainty is a function of record-to-record (RTR) uncertainty, design requirements related (DR) uncertainty, test data-related (TD) uncertainty, and modeling (MDL) uncertainty. Values of total system collapse uncertainty,  $\beta_{TOT}$  are provided in Table 7-2 of the ATC-63. Table 7-3 of the ATC-63 provides acceptable values of adjusted collapse margin ratio,  $ACMR_{10\%}$  and  $ACMR_{20\%}$ , based on total system collapse uncertainty and values of acceptable collapse probability, taken as 10% and 20%, respectively.

Figure 12 shows the response spectra of the earthquake records used in the incremental dynamic analyses along with the median response spectrum and the MCE design spectrum. The ground motions are scaled in such a way that the median spectral acceleration of the record set matches the MCE design spectral acceleration at the fundamental period of the model structure. Fig. 13 depicts the incremental dynamic analysis results of the Y-Type 3 structure. The median collapse intensity,  $\hat{S}_{CT}$ , and the MCE intensity,  $S_{MT}$ , are also shown in the figure, which are 0.35 and 0.07, respectively. This results in the collapse margin ratio (CMR) of 5.0. From Table 7-2 of the ATC-63 the total system collapse uncertainty,  $\beta_{TOT}$ , of the model structure is obtained as 0.725. Using the fundamental period, 3.28 sec., and ductility capacity obtained from push-over analysis, 2.07, the spectral shape factor,  $SSF$ , is obtained as 1.15 which is multiplied to the CMR to obtain the adjusted collapse margin ratio (ACMR) of 5.87. This value is significantly larger than the acceptable value of the adjusted collapse margin ratio,  $ACMR_{20\%}$ , provided in the Table 7-3 of the ATC-63, which is 1.84.

The seismic fragility is described by the conditional probability that the structural capacity,  $C$ , fails to resist



**Figure 12.** Response spectra for the record set and intensity anchoring to the MCE design spectrum corresponding to the fundamental natural period of the Y-type 3 model structure.



**Figure 13.** Maximum inter-story drifts of Y type-3 analysis model obtained from incremental dynamic analysis.

the structural demand,  $D$ , given the seismic intensity hazard,  $SI$ , and is modeled by a lognormal cumulative distribution function as follows (Celik and Ellingwood, 2009):

$$P[C < D | SI = x] = 1 - \Phi \left[ \frac{\ln(\hat{C}/\hat{D})}{\sqrt{\beta_{D|SI}^2 + \beta_C^2 + \beta_M^2}} \right] \quad (3)$$

where  $\Phi[\cdot]$  = Standard normal probability integral,  $\hat{C}$  = median structural capacity, associated with the limit state,  $\hat{D}$  = median structural demand,  $\beta_{D|SI}$  = uncertainty in  $D$ ,  $\beta_C$  = uncertainty in  $C$ ,  $\beta_M$  = modeling uncertainty. Fig. 14 depicts the fragility curves of the Y-Type 3 analysis model

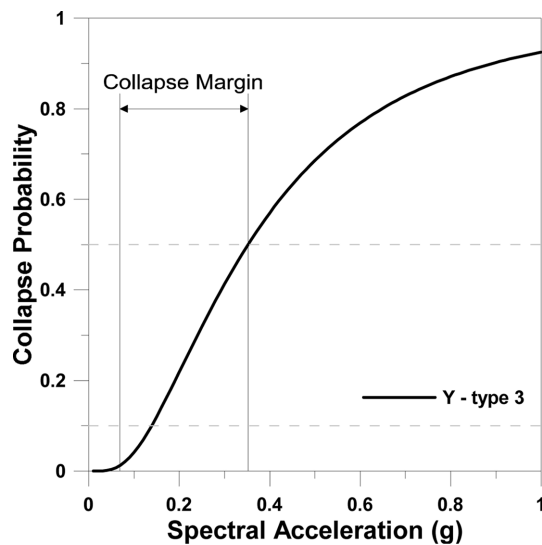


**Figure 14.** Fragility curve of the model structure obtained from twenty two pairs of earthquake records.

structure obtained from IDA results of the 22 pairs of ground motions. The total system collapse uncertainty,  $\beta_{TOT}$ , which was used to obtain the acceptable values of adjusted collapse margin ratio in the previous section, was used for the uncertainty in the normal probability integral function  $\Phi$ . The margin for collapse, which was defined as the difference between the MCE ground motion and the spectral accelerations corresponding to the 50% probability of collapse, was also indicated in the figure. It can be observed that the collapse probability of the structure reached 0.5 when the response spectrum of input earthquake is 0.35 g which is significantly larger than the response spectrum of the MCE-level earthquake of 0.07 g. It is recommended in the ATC-63 that the probability of collapse for the MCE-level earthquake be less than 10%, which is satisfied in this example.

## 5. Conclusions

This study investigated the seismic performances of apartment buildings with Y- and box-shaped plans having central core. Three types of model structures were designed for each shape depending on the amount of shear partition walls: structures with all shear walls, structures with all columns except the core walls, and structures with shear walls and columns combined. Nonlinear static and dynamic analyses were carried out to compare the structural performances of the model structures with different amount of shear partition walls.

The required amount of concrete to satisfy the specified design loads was the largest in the all shear wall structures, and decreased as more and more shear walls were replaced with columns. The amount of re-bars increased significantly in the structures with columns. According to nonlinear static and dynamic analysis results, the struc-

tures with all shear walls and all columns turned out to have the largest and the smallest strengths, respectively. However it was observed that even the all-column structures with central core also had proper load resisting capacity for design level seismic load. The fragility analysis of the Y-Type 3 structure, which showed smallest stiffness and strength in the nonlinear static and dynamic analyses, indicated that the probability of collapse for the MCE-level earthquake was less than 10%, which satisfies the recommendation of the ATC-63. Based on the seismic performance and the structural materials used to satisfy the design loads, it was concluded that the structure with a central core and the columns replacing partition shear walls could be an efficient structure system for residential buildings with enhanced freedom of spatial variability. It was also concluded that the Type 2 structures with mixed shear walls and interior columns could be the most economical structure in terms of the amount of structural material.

## Acknowledgements

This research was supported by a grant (13AUDP-B06 6083-01) from Architecture & Urban Development Research Program funded by Ministry of Land, Infrastructure and Transport of Korean government.

## References

- ASCE, Seismic Rehabilitation of Existing Buildings, ASCE Standard ASCE/SEI 41-06, American Society of Civil Engineers, Reston, Virginia.
- Barbat A. H., L. G. Pujades, and N. Lantada (2008), Seismic damage evaluation in urban areas using the capacity spectrum method: Application to barcelona, *Soil Dynamics and Earthquake Engineering*, 28, pp. 851–865.
- Dazio, A., Beyer, K., Bachmann, H. (2009). “Quasi-static Cyclic Tests and Plastic Hinge Analysis of RC Structural Walls”, *Engineering Structures*, 31, pp. 1556–1571.
- FEMA (1999). HAZUS99 Technical Manual.
- Gupta, A. and Rangan, B. V. (1998). High-strength concrete (HSC) structural walls, *ACI Structural Journal*, 95(2), pp. 194–204.
- ICC. (2009) International building code. Falls Church (Virginia, USA): International Code Council.
- Kara, I. F. and Dundar, C. (2009), Prediction of deflection of reinforced concrete shear walls. *Adv. Eng. Softw.*, 40, pp. 777–785.
- Kim, H, Lee, D., and Kim, C. (2005). Efficient three dimensional seismic analysis of a high-rise building structure with shear walls. *Eng. Struct.*, 27(6), pp. 963–976.
- KBC (2009). Design codes for building structures, Korea Architectural Institute, Seoul, Korea.
- Kim, J., Lee, J., and Han, S. (2013). Seismic Performance of Building Structures with Spatial Variability, *International Journal of Engineering and Technology*, 5(6), pp. page.
- Lee, J. and Kim, J. (2013). Seismic performance evaluation of staggered wall structures using Fema P695 procedure,

- Magazine of Concrete Research*, 65(17), pp. 1023~1033.
- MIDAS GENW. (2011). General Structure Design System for Window, Ver. 7.9.5.
- Mo, Y. L., Zhong, J., and Hsu, T. T. C. (2008). "Seismic simulation of RC wall-type structures," *Eng. Struct.*, 30, pp. 3167~3175.
- Paulay T. and Priestley M. J. N. (1992) Seismic Design of Reinforced Concrete and Masonry Buildings.
- PEER NGA Data Base, <http://peer.berkeley.edu/nga/>
- Perform3D. (2006). Nonlinear Analysis and Performance Assessment for 3D Structures-User Guide, Computers & Structures, Inc., Berkeley, CA.
- Thomsen, I. V., J. H., and Wallace, W. J. (2004). "Displacement-Based Design of Slender Reinforced Concrete Structural Walls-Experimental Verification," *Journal of Structural Engineering*, 130(4), ASCE.
- Vamvatsikos, D. and Cornell, C. A. (2002). "Incremental dynamic analysis," *Earthquake Engineering and Structural Dynamics*, 31(3), pp. 491~514.
- Wdowicki, J. and Wdowicka, E. (2012). "Analysis of shear wall structures of variable cross section," *The Structural Design of Tall and Special Buildings*, 21(1), pp. 1~15.
- Yun, H. D., Choi, C. S., and Lee, L. H. (2004). "Earthquake performance of high-strength concrete structural walls with boundary elements," 13th World Conference on Earthquake Engineering, Vancouver, B.C., Canada.